

INFLUENCE OF DAMAGE ON CREEP BUCKLING OF A STRUT

JERZY BIAŁKIEWICZ

Division of Solid Mechanics, Chalmers University of Technology, Gothenburg, Sweden†

(Received 27 June 1979; in revised form 6 December 1979)

Abstract—Theoretical analyses of the title problem are presented. Two simple mechanical models of a strut are considered: hinge and sandwich. The analyses consist of two phases: instantaneous load application and creep and damage under constant load. The influence on the buckling time of the load, the initial deflection and the material properties as reflected in the analytical form of constitutive equations is numerically examined.

1. INTRODUCTION

Theoretical analyses of the behaviour of a compressive rod will be presented. The material model is assumed as nonlinear viscoelastic (Norton creep) with influence of Kachanov-Rabotnov type damage. This description of creep buckling of a strut is due to P. O. Boström [1, 2]. An instability surface can be defined in the load-deflection-damage space. If the instability surface is reached by the state point of the strut, buckling takes place. The load history can be an arbitrary function of time. A load history according to the Heaviside function will be applied below. In this case the process will be divided into two phases: an instantaneous load application phase and an ensuing creep phase under constant load. Each of them can separately lead to instability. The behaviour of the strut is analysed using two mechanical models: a hinge model and a sandwich model. In both cases strains and damage are localized at the midspan cross section of the strut.

The governing set of equations will be formulated in dimensionless variables. The influence on the buckling time of the load, the initial deflection and the material properties is numerically examined.

2. TWO MECHANICAL MODELS

Creep and damage separately lead to strongly nonlinear relations between strain rate and stress. Simultaneous presence of creep deformation and damage will enhance this nonlinearity. Hence a rod subject to axial loading will take a quite pointed shape. The simplest approximation of the mechanical behaviour of the rod can be obtained by taking a model which contains two rigid rods joined by a hinge [3]. Initial and deformed states of the hinge model are shown in Fig. 1(a).

The hinge is characterized by a relation between the bending moment M and the angular deflection ϕ . Assuming small values of the angle α (Fig. 1a) those magnitudes can be written as

$$M = PL\alpha \quad (2.1)$$

$$\phi = 2\alpha - 2\alpha_{00} \quad (2.2)$$

where α_{00} denotes the angle of initial deflection of the rod before load application. The effective dimensionless bending moment considering damage will take the form

$$\bar{\mu} = \frac{M}{\mu_0(1-\omega)} \quad (2.3)$$

where ω denotes the damage and μ_0 is a constant introduced for dimensional purposes.

†Present Address: Department of Civil Engineering, Technical University, Cracow, Poland.

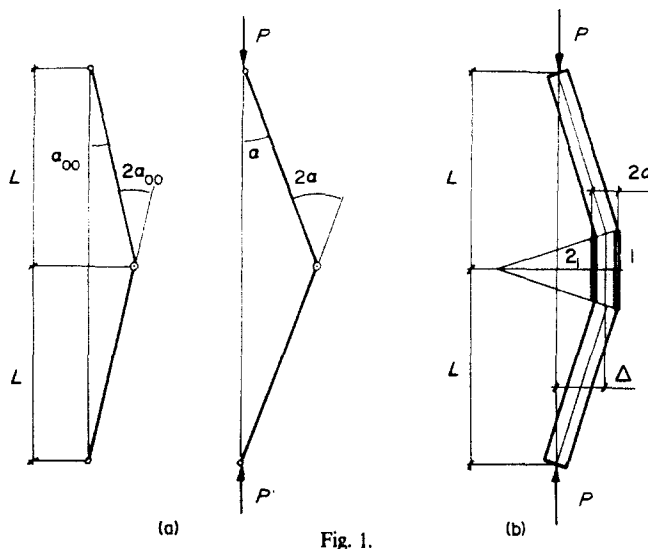


Fig. 1.

Introduction of M into (2.3) according to (2.1) yields the following relation

$$\bar{\mu} = \frac{PL\alpha}{\mu_0(1-\omega)} = \bar{M} \frac{\alpha}{1-\omega} \tag{2.4}$$

where \bar{M} is defined as

$$\bar{M} = \frac{PL}{\mu_0} \tag{2.5}$$

The quantity \bar{M} will characterize the value of external load for the hinge model.

A more accurate model of a compressed rod is a sandwich model (Shanley model)[4-6]. In this model all deformation occurs in two thin flanges, 1 and 2, see Fig. 1(b), which carry only axial loads. The sandwich model takes into account the difference in damage behaviour under tension and compression. If the forces in the flanges are denoted Q_1 and Q_2 , equilibrium requires

$$Q_1 = -P \frac{d-\Delta}{2d} \tag{2.6}$$

$$Q_2 = -P \frac{d+\Delta}{2d} \tag{2.7}$$

where Δ is the deflection, $2d$ is the diameter of the rod and P is the compressive load. Hence Q_2 will be compressive for all deflections, whereas Q_1 will change from compressive into tensile, when Δ exceeds d . Damage therefore will occur in flange 1 only for $\Delta > d$. Denoting by $A/2$ the cross sectional area of each flange dimensionless stresses can be written as

$$\bar{s}_1 = -\frac{P}{As_0} \frac{1-\frac{\Delta}{d}}{1-\omega_1} \tag{2.8}$$

$$\bar{s}_2 = -\frac{P}{As_0} \left(1 + \frac{\Delta}{d}\right) \tag{2.9}$$

where ω_1 is the damage in flange 1 and s_0 is a constant introduced for dimensional purposes.

Introducing here

$$\bar{P} = \frac{P}{As_0} \tag{2.10}$$

$$\bar{\Delta} = \frac{\Delta}{d} \tag{2.11}$$

which characterize the external load and the deflection for the sandwich model the expressions (2.8) and (2.9) can be written in the following form

$$\bar{s}_1 = -\bar{P} \frac{1-\bar{\Delta}}{1-\omega_1} \tag{2.12}$$

$$\bar{s}_2 = -\bar{P}(1+\bar{\Delta}). \tag{2.13}$$

Below the solution for each model of a rod will be presented separately.

3. BUCKLING OF ROD—HINGE MODEL

For the hinge model the constitutive equations describing the creep and damage[7] in dimensionless variables are taken as

$$\frac{d\phi}{d\tau} = G'(\bar{\mu})\frac{d\bar{\mu}}{d\tau} + F(\bar{\mu}) \tag{3.1}$$

$$\frac{d\omega}{d\tau} = g'(\bar{\mu})\frac{d\bar{\mu}}{d\tau} + f(\bar{\mu}). \tag{3.2}$$

Dimensionless time τ is here expressed by

$$\tau = \frac{t}{t_0} \tag{3.3}$$

where t denotes real time and t_0 is a constant introduced for dimensional purposes. The functions G, F, g and f are usually found to be nonlinear. In this paper they are taken as power functions

$$\begin{aligned} G(\bar{\mu}) &= A\bar{\mu}^\eta \\ g(\bar{\mu}) &= C\bar{\mu}^\gamma \\ F(\bar{\mu}) &= \frac{B}{t_0} \bar{\mu}^\beta \\ f(\bar{\mu}) &= \frac{D}{t_0} \bar{\mu}^\delta \end{aligned} \tag{3.4}$$

From eqns (3.1), (3.2) and (2.4), (3.4) the governing set of equations follow which can be written in the form

$$Rd\alpha = Sd\bar{M} + Td\tau \tag{3.5}$$

$$Rd\omega = Ud\bar{M} + Vd\tau. \tag{3.6}$$

Here the functions R, S, T, U and V are given by

$$R = 2 - \frac{2C\gamma}{1-\omega} \left(\frac{\bar{M}\alpha}{1-\omega}\right)^\gamma - \frac{A\eta}{\alpha} \left(\frac{\bar{M}\alpha}{1-\omega}\right)^\eta \tag{3.7}$$

$$S = \frac{\eta A}{\bar{M}} \left(\frac{\bar{M}\alpha}{1-\omega}\right)^\eta \tag{3.8}$$

$$T = B \left(\frac{\bar{M}\alpha}{1-\omega}\right)^\beta + \frac{AD\eta}{1-\omega} \left(\frac{\bar{M}\alpha}{1-\omega}\right)^{\eta+\delta} - \frac{BC\gamma}{1-\omega} \left(\frac{\bar{M}\alpha}{1-\omega}\right)^{\beta+\gamma} \tag{3.9}$$

$$U = \frac{2\gamma C}{\bar{M}} \left(\frac{\bar{M}\alpha}{1-\omega}\right)^\gamma \tag{3.10}$$

$$V = 2D \left(\frac{\bar{M}\alpha}{1-\omega}\right)^\delta + \frac{CB\gamma}{\alpha} \left(\frac{\bar{M}\alpha}{1-\omega}\right)^{\beta+\gamma-1} - \frac{AD\eta}{\alpha} \left(\frac{\bar{M}\alpha}{1-\omega}\right)^{\delta+\eta}. \tag{3.11}$$

Below, in the numerical analyses of buckling of the compressed rod at elevated temperatures, the constants describing the properties of the rod will be taken as follows

$$\begin{aligned} A = 0.01 & \quad B/t_0 = 0.1 & \quad C = 0.1 & \quad D/t_0 = 1.0 \\ \eta = 1 & \quad \beta = 7 & \quad \gamma = 1 & \quad \delta = 5. \end{aligned} \quad (3.12)$$

These data correspond to creep and damage behaviour, typical of many metals used in high temperature applications.

A standard type of loading history in creep buckling studies is step loading

$$\bar{M}(\tau) = \bar{M}_0 H(\tau) \quad (3.13)$$

where $H(\tau)$ is the Heaviside unit step function. In this case two phases can be distinguished: an instantaneous load application phase and a phase under constant load.

The instability surface in load-deflection-damage space for both phases has the equation

$$R = 2 - \frac{2C\gamma}{1-\omega} \left(\frac{\bar{M}\alpha}{1-\omega} \right)^\gamma - \frac{A\eta}{\alpha} \left(\frac{\bar{M}\alpha}{1-\omega} \right)^\eta = 0. \quad (3.14)$$

The load application phase will first be examined. In this case the governing set of equations takes the form

$$d\alpha/d\bar{M} = S/R \quad (3.15)$$

$$d\omega/d\bar{M} = U/R. \quad (3.16)$$

The solution of the set of differential eqns (3.15) and (3.16) will be determined applying a higher order Runge-Kutta method. The initial conditions for the functions $\alpha(\bar{M})$ and $\omega(\bar{M})$ can be written

$$\alpha(0) = \alpha_{00} \quad \omega(0) = 0. \quad (3.17)$$

Numerical integration of the eqns (3.15) and (3.16) with initial conditions (3.17) will be carried out until the state point \bar{M} , $\alpha(\bar{M})$, $\omega(\bar{M})$ reaches the instability surface $R = 0$ defined by (3.14). From eqns (3.15) and (3.16) follows that loss of equilibrium in the sense $d\alpha/d\bar{M} \rightarrow \infty$ and $d\omega/d\bar{M} \rightarrow \infty$ is reached at the surface $R = 0$. The initial conditions (3.17) suggest analysing the influence of initial deflection α_{00} on the value of load \bar{M} , deflection α , and damage parameter ω at instability.

Illustrative solutions are presented in Figs. 2, 3 and 4. Continuous lines are connected with load application. Dashed lines are instability curves in the ω - P , α - P , ω - α planes. It is obvious that with increasing values of initial deflection α_{00} the critical value of the load \bar{M} is decreasing. It is seen from Fig. 2 that the critical damage in a buckling problem increases with increasing initial deflection. For fixed material constants (3.12) the limit value of critical damage is equal to 0.5. From Fig. 3 follows that for $\alpha_{00} > 0.02$ instantaneous buckling takes place for approximately the same growth of deflection $\Delta\alpha = 0.02$.

The relations in the ω - α plane are shown in Fig. 4. The functions $\alpha = \alpha(\omega)$ in instantaneous loading for different values of initial deflection are linear because the exponents α and γ are taken as equal to one. Additionally in Fig. 4 the instability line is presented for the case $A = 0$ (instantaneous, pure damage buckling). For the chosen values of the material constants the magnitude of damage in instantaneous buckling in this case does not depend on the initial deflection of the rod. Instantaneous buckling here always takes place when $\omega = 0.5$. This line is the asymptote for the buckling curve when instantaneous deflections occur ($A \neq 0$).

If the load \bar{M}_0 is less than the value which causes instantaneous buckling, a stable state will arise and a creep phase will follow. With the load history (3.13) the differential equations

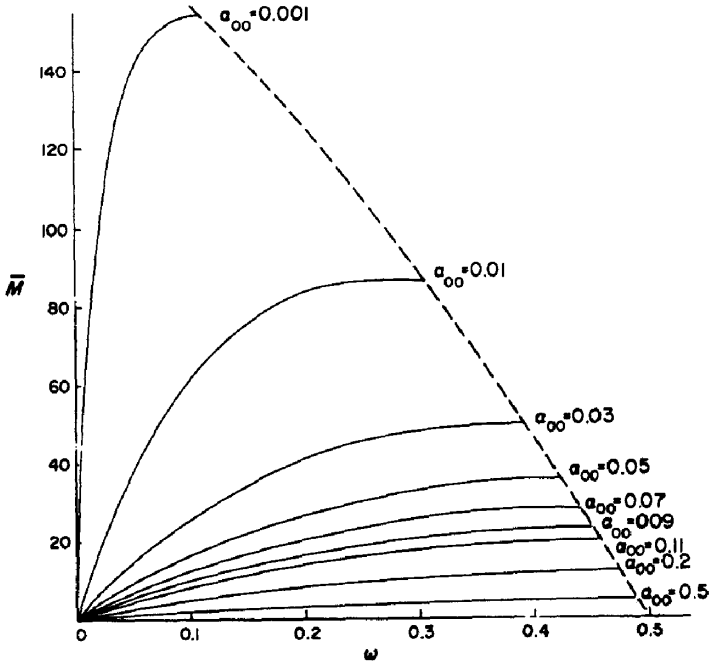


Fig. 2.

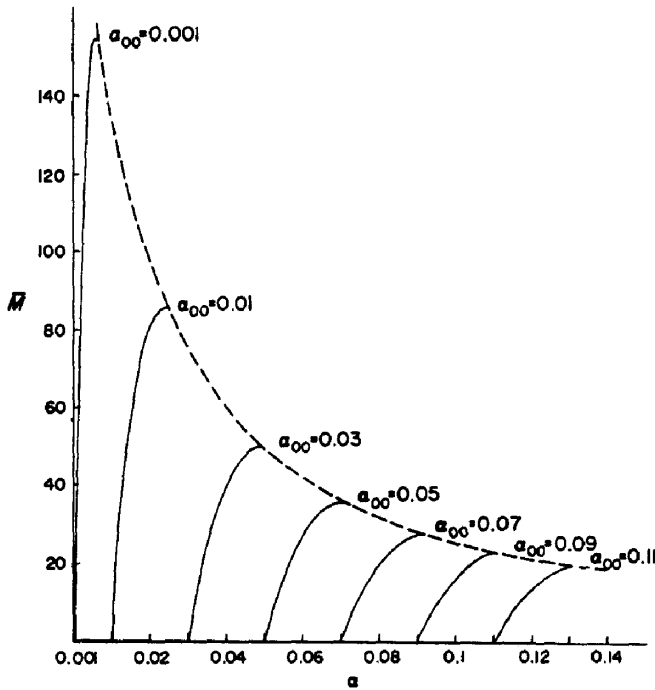


Fig. 3.

describing the creep phase take the form

$$d\alpha/d\tau = T/R \tag{3.18}$$

$$d\omega/d\tau = V/R. \tag{3.19}$$

The initial conditions for the functions $\alpha(\tau)$ and $\omega(\tau)$ take the form

$$\alpha(0) = \alpha_0 \quad \omega(0) = \omega_0. \tag{3.20}$$

Here α_0 and ω_0 are the hinge angle and damage which have been achieved in the instantaneous load application phase. The creep buckling time will be obtained as the time when $R = 0$. From

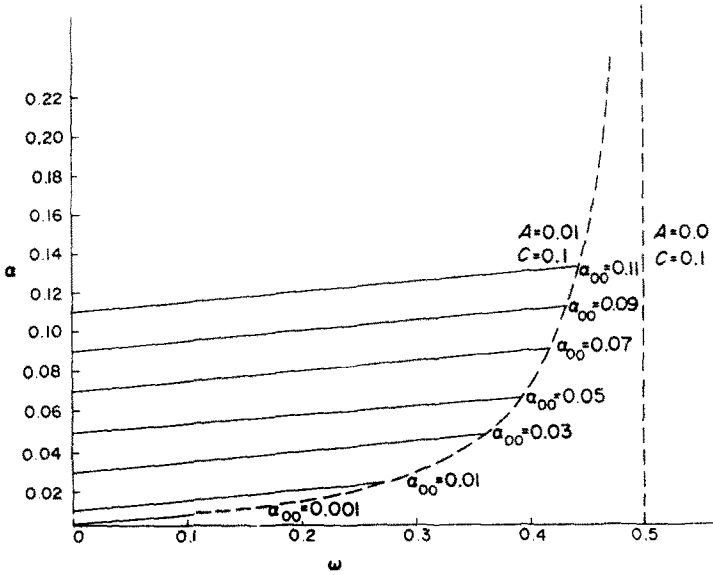


Fig. 4.

(3.18) and (3.19) follows that creep buckling in the dense $d\alpha/d\tau \rightarrow \infty$ and $d\omega/d\tau \rightarrow \infty$ is obtained when the state point $\bar{M}_0, \alpha(\tau), \omega(\tau)$ reaches the instability surface defined by (3.14).

First the influence of the load \bar{M}_0 on the shape of the functions α and ω will be examined. An illustrative solution is shown in Fig. 5 when the initial deflection is $\alpha_{00} = 0.01$. A thick continuous line shows the conditions for instantaneous buckling when $\bar{M}_0 = 86$ (point $H_9 = E_9$). Points H_i (for $i = 1 \dots 8$) on this line show the ends of the instantaneous load application phase and the beginning of creep phase. The initial conditions (3.20) are described by the co-ordinates of points H_i . Thin continuous lines show the relation between deflection α and damage ω in the ensuing creep phase. Buckling will occur in points E_i which define the instability curve in the

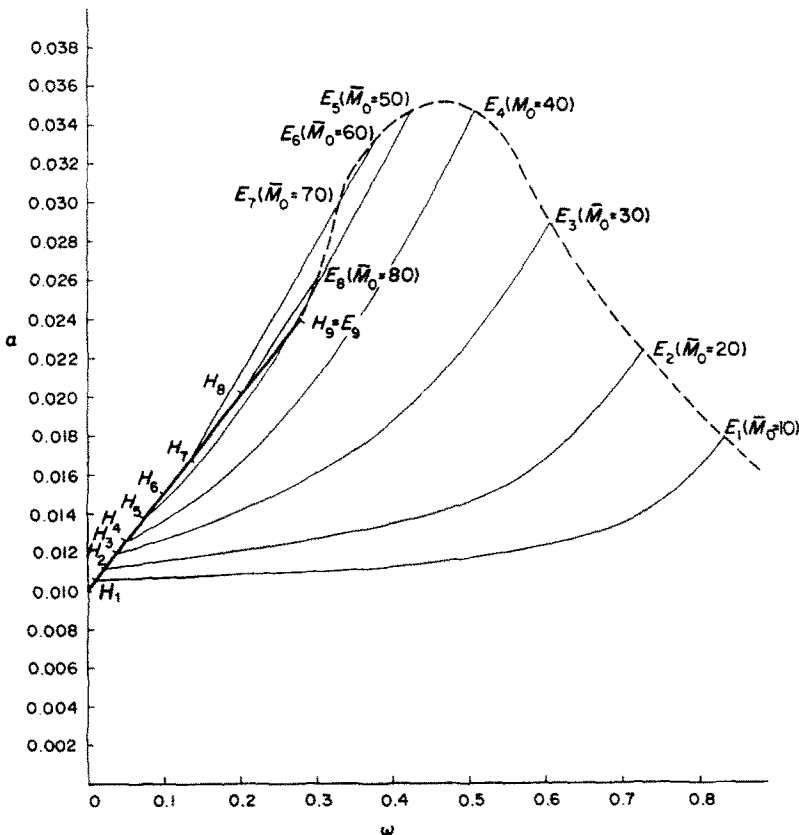


Fig. 5.

ω - α plane (dashed line). The instability curve achieves a maximum value at the angular deflection which causes instability in the load region $\bar{M}_0 = 40$ –50. From Fig. 5 it seems that the magnitude of damage will increase during creep buckling when the load value \bar{M}_0 is decreased. Simultaneously the critical deflection at creep buckling decreases with decreasing load. The transition from a ductile brittle buckling to a purely brittle buckling is shown in Table 1 and in Fig. 6. The solutions when the initial deflection $\alpha_{00} = 0.01$ and the load $\bar{M}_0 = 30$ are presented here.

The solutions have the following interpretation: $A = 0$ —no deformation in instantaneous load application; $B = 0$ —no deformation in the creep phase; $A = B = 0$ —no deformation at all (pure brittle buckling). The assumption $A = 0$ has a particularly large influence on the change of the function $\alpha = \alpha(\omega)$ (from $A \neq 0$ and $B \neq 0$). Pure brittle buckling occurs when $\omega \rightarrow 1$ and when the initial deflection $\alpha_{00} \rightarrow 0$. In Fig. 6, analogous to Fig. 5, the points H_i determine the beginning and E_i the end of the creep phase.

4. BUCKLING OF ROD—SANDWICH MODEL

In this case the governing set of equations are different for flange 1 and flange 2. In dimensionless form they can be written

$$\frac{d\epsilon_1}{d\tau} = G'(\bar{s}_1) \frac{d\bar{s}_1}{d\tau} H(\bar{s}_1 \cdot \dot{\bar{s}}_1) + F(\bar{s}_1) \quad (4.1)$$

$$\frac{d\epsilon_2}{d\tau} = G'(\bar{s}_2) \frac{d\bar{s}_2}{d\tau} + F(\bar{s}_2) \quad (4.2)$$

$$\frac{d\omega_1}{d\tau} = g'(\bar{s}_1) \frac{d\bar{s}_1}{d\tau} H(\bar{s}_1) + f(\bar{s}_1) H(\bar{s}_1) \quad (4.3)$$

$$\omega_2 = 0. \quad (4.4)$$

Here ϵ_1 and ϵ_2 are the strains in flanges 1 and 2 respectively. The Heaviside functions $H(\bar{s}_1)$ and $H(\bar{s}_1 \cdot \dot{\bar{s}}_1)$ describe the damage and strain behaviour in flange 1 under compression and unloading respectively. Compatibility requires

$$\epsilon_1 - \epsilon_2 = \frac{\bar{\Delta} - \bar{\Delta}_{00}}{\lambda} \quad (4.5)$$

where $\bar{\Delta}_{00}$ is the dimensionless initial deflection, and

$$\lambda = \frac{hL}{2d^2} \quad (4.6)$$

is a dimensionless constant which characterizes the geometry of the rod. The form of the functions G , F , g and f is taken analogous as for the hinge model (3.4) formally substituting the bending moment $\bar{\mu}$ by stresses \bar{s}_1 or \bar{s}_2 . Utilizing the compatibility condition (4.5) the governing

Table 1.

A	$\frac{B}{I_0}$	Buckling time ($C = 0.1, D/I_0 = 1$)
0.01	0.1	13.2
0.0	0.1	38.7
0.01	0.0	20.4
0.0	0.0	57.7

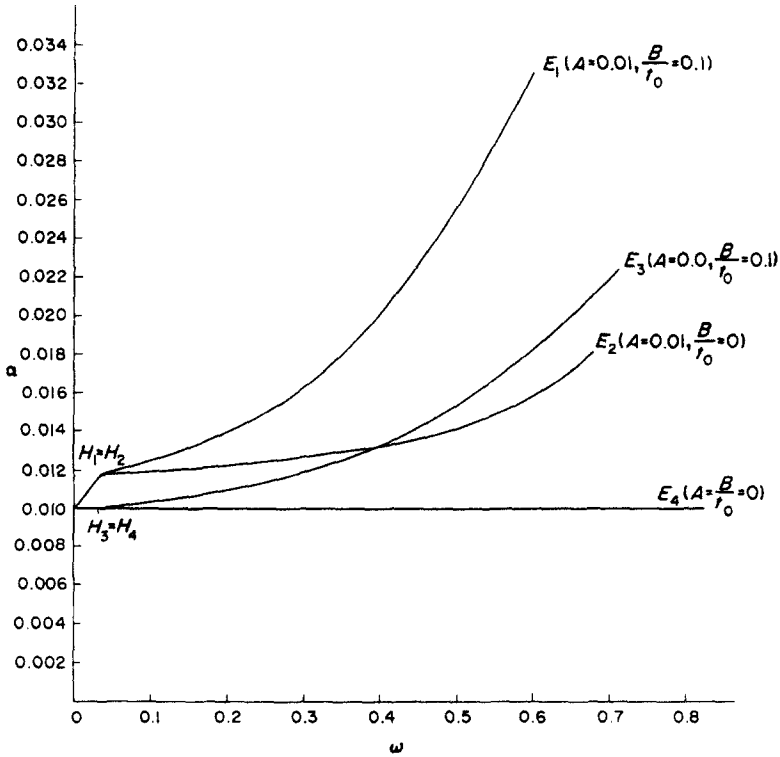


Fig. 6.

set of eqns (4.1)–(4.3) after insertion of (2.10) and (2.11) can be written

$$Ed\bar{\Delta} = Id\bar{P} + Jd\tau \tag{4.7}$$

$$Ed\omega_1 = Kd\bar{P} + Nd\tau. \tag{4.8}$$

Here the functions E, I, J, K and N are given by

$$E = (1 - \lambda\bar{P}A\eta\bar{s}_2^{\gamma-1})[1 - \omega_1 - C\gamma\bar{s}_1^\gamma H(\bar{s}_1)] - \lambda\bar{P}A\eta\bar{s}_1^{\gamma-1}H(\bar{s}_1 \cdot \bar{s}_1) \tag{4.9}$$

$$I = \lambda\frac{A}{\bar{P}}\eta[\bar{s}_1^\gamma(1 - \omega_1)H(\bar{s}_1 \cdot \bar{s}_1) - \bar{s}_2^\gamma(1 - \omega_1 - C\gamma\bar{s}_1^\gamma H(\bar{s}_1))] \tag{4.10}$$

$$J = \lambda AD\eta\bar{s}_1^{\gamma+\delta}H(\bar{s}_1) + B(\bar{s}_1^\beta - \bar{s}_2^\beta)[1 - \omega_1 - C\gamma\bar{s}_1^\gamma H(\bar{s}_1)] \tag{4.11}$$

$$K = \frac{C\gamma\bar{s}_1^\gamma}{\bar{P}}H(\bar{s}_1)[(1 - \omega_1)(1 - \lambda\bar{P}A\eta\bar{s}_2^{\gamma-1}) - A\eta\frac{\bar{s}_2^\gamma}{\bar{s}_1}\bar{P}\lambda] \tag{4.12}$$

$$N = \lambda H(\bar{s}_1)[CB\gamma(\bar{s}_1^\beta - \bar{s}_2^\beta)\bar{P}\bar{s}_1^{\gamma-1} - DA\eta\bar{P}\bar{s}_1^{\gamma+\delta-1} + \frac{1-\omega_1}{\lambda}D\bar{s}_1^\delta(1 - \gamma\bar{P}A\eta\bar{s}_2^{\gamma-1})]. \tag{4.13}$$

The functions \bar{s}_1 and \bar{s}_2 are defined by expressions (2.12) and (2.13). The governing equations will be analysed for the case of step loading

$$\bar{P} = \bar{P}_0H(\tau). \tag{4.14}$$

Assuming the same material data as for the hinge model viz (3.12) and $\lambda = 25$ the load application phase will first be studied.

For load application equations (4.7) and (4.8) take the form

$$d\bar{\Delta}/d\bar{P} = I/E \tag{4.15}$$

$$d\omega_1/d\bar{P} = K/E \tag{4.16}$$

with initial conditions

$$\bar{\Delta}(0) = \bar{\Delta}_{00} \quad \omega_1(0) = 0. \tag{4.17}$$

In this case the instability surface in the load-deflection-damage space has the equation

$$E = (1 - \gamma \bar{P} A \eta \bar{s}_2^{\gamma-1}) [1 - \omega_1 - C \gamma \bar{s}_1^\gamma H(\bar{s}_1)] - \lambda \bar{P} A \eta \bar{s}_1^{\gamma-1} H(\bar{s}_1 \cdot \dot{\bar{s}}_1) = 0. \tag{4.18}$$

The stress \bar{s}_2 will be compressive for all deflections $\bar{\Delta}$ and therefore $\omega_2 = 0$. The stress \bar{s}_1 will change from compressive into tensile, when $\bar{\Delta}$ exceeds 1. This implies that damage creation will start in flange 1 at this instant. The dependence of net stress in flange 1 on the external load \bar{P} for different values of initial deflection $\bar{\Delta}_{00}$ is presented in Fig. 7. The instability curve in the $\bar{P}-\bar{s}_1$ plane is shown by a dashed line. For initial deflection $\bar{\Delta}_{00}$ in the interval 0.22–1.0 the sign of \bar{s}_1 changes from compressive into tensile. In the limiting case $\bar{\Delta}_{00} \approx 0.22$ buckling occurs when \bar{s}_1 changes sign. For initial deflection $\bar{\Delta}_{00} \leq 0.22$ instantaneous buckling is purely ductile.

The relation between the load, the damage ω_1 and the deflection $\bar{\Delta}$ for different initial deflections $\bar{\Delta}_{00}$ is shown in Figs. 8 and 9. Continuous lines are connected with loading, whereas dashed lines show the buckling curves. The starting points for the functions $\bar{P} = \bar{P}(\omega_1)$ are different (see Fig. 8) when the initial deflection $\Delta_{00} < 1$. They are connected with the change of

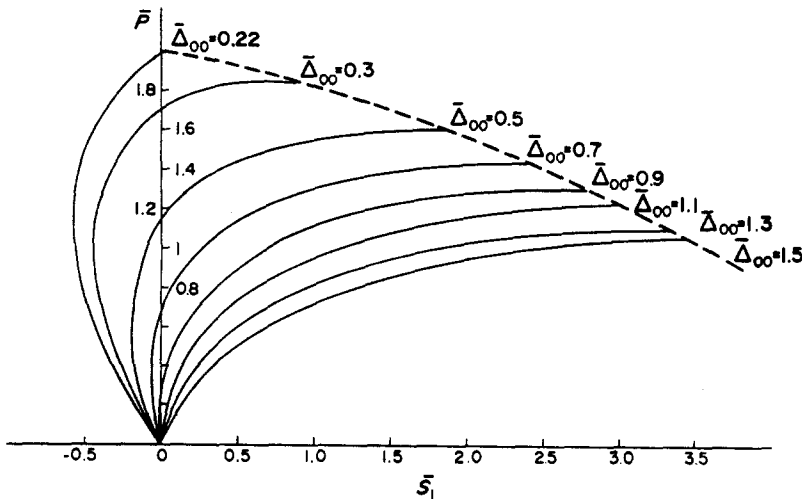


Fig. 7.

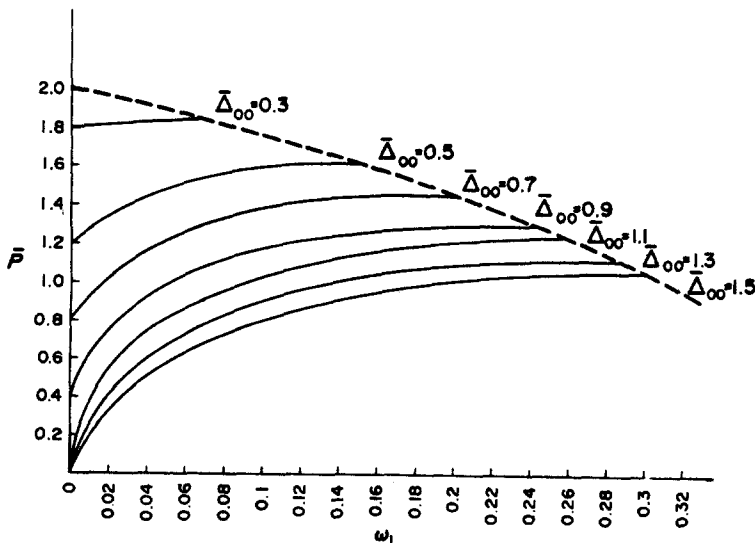


Fig. 8.

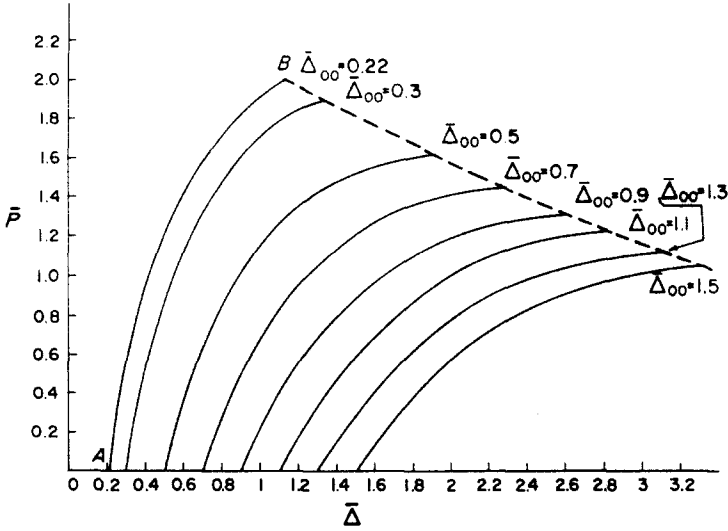


Fig. 9.

the sign of stresses \bar{s}_1 from negative into positive. On the left side of the curve AB , Fig. 9, instantaneous buckling occurs without damage creation $\bar{\Delta}_{00} \leq 0.22$). If the load \bar{P}_0 is less than the value which causes instantaneous buckling a creep phase will occur.

The governing equations for this creep phase take the form

$$d\bar{\Delta}/d\tau = I/E \tag{4.19}$$

$$d\omega_1/d\tau = N/E. \tag{4.20}$$

Initial conditions for the functions $\bar{\Delta}(\tau)$ and $\omega_1(\tau)$ are determined by the previous instantaneous load application, viz

$$\bar{\Delta}(0) = \bar{\Delta}_0 \quad \omega_1(0) = \omega_{1,0}. \tag{4.21}$$

First the influence of the load \bar{P}_0 on the critical magnitudes $\bar{\Delta}$ and ω_1 is examined. The solution with initial deflection $\Delta_{00} = 0.7$ is shown in Fig. 10. Instantaneous buckling (thick line occurs in

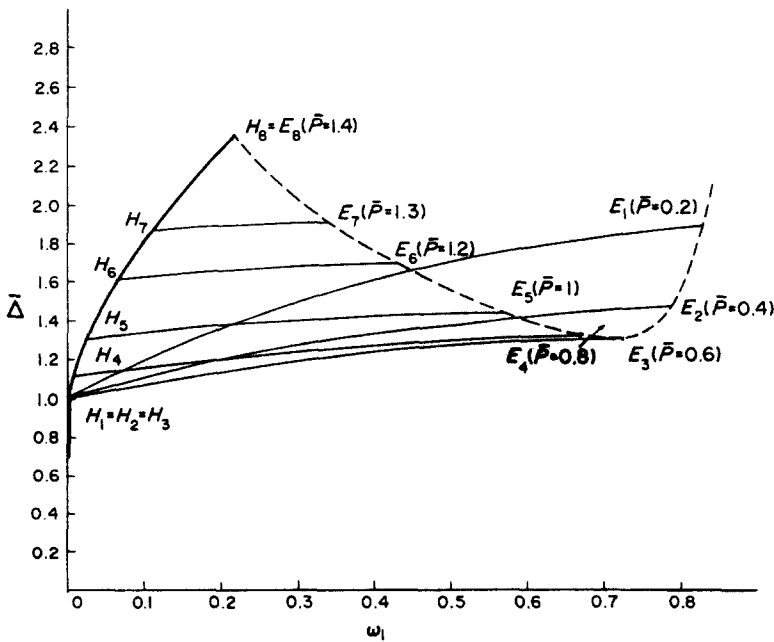


Fig. 10.

Table 2.

A	$\frac{B}{t_0}$	Buckling time ($C = 0.1, D/t_0 = 1$)
0.01	0.1	$6.2 \cdot 10^{-2}$
0.0	0.1	$4.1 \cdot 10^{-1}$
0.01	0.0	$3.6 \cdot 10^1$
0.0	0.0	$2.2 \cdot 10^5$

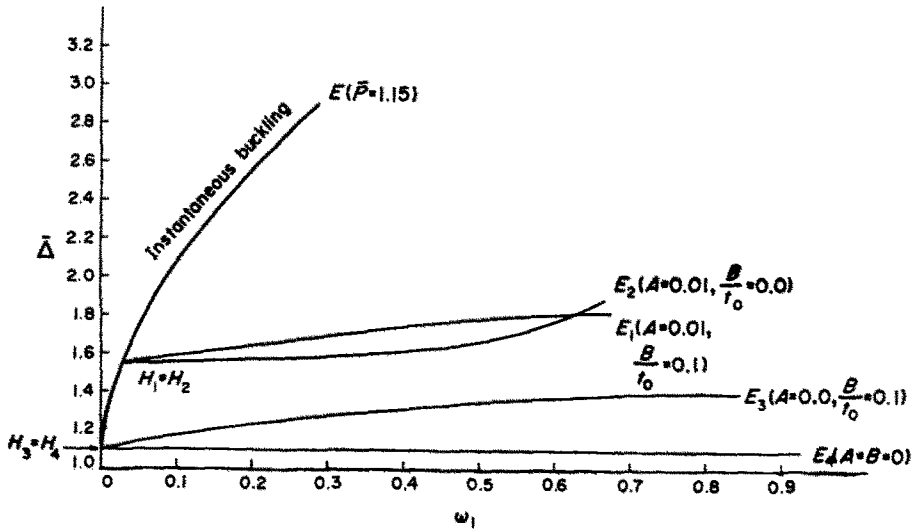


Fig. 11.

the point $H_8 = E_8$ which is connected with the load $\bar{P}_0 = 1.4$. Points H_i ($i = 1 \dots 7$) define initial conditions (4.21) for different values of the load \bar{P}_0 less than 1.4. The creep phase is presented by the thin lines. Creep buckling occurs in points E_i . These points define the dashed instability curve. If the deflection, reached in instantaneous load application, was less or equal to one, growth of damage in the creep phase starts from the point $\bar{\Delta} = 1$ (points H_1, H_2, H_3). The instability curve has a minimum for $\bar{P}_0 = 0.6$.

Comparison between Fig. 5 and Fig. 10 shows that a maximum in the instability curve for the hinge model corresponds to a minimum in the instability curve for the sandwich model. For initial deflections $\bar{\Delta}_0 > 1$ the deflection in the sandwich model will increase very little in the creep phase in contrast to the hinge model.

A similar transition as for the hinge model from ductile-brittle buckling to purely brittle buckling is shown in Table 2 and in Fig. 11. In these cases are illustrated solutions for initial deflection $\bar{\Delta}_{00} = 1.1$ and load $\bar{P}_0 = 0.6$. The solutions have the same interpretation as for the hinge model. The influence of assumptions of material data on buckling time is particularly presented in Table 2. The relation between ω_1 and $\bar{\Delta}$ is shown in Fig. 11.

5. FINAL REMARKS

The numerical analysis indicates different behaviour of a rod depending on the assumed mechanical model (hinge or sandwich). For materials displaying no deformation, instantaneous or delayed, instability is reached at a finite load or after a finite time. Hence no observable change in configuration occurs before equilibrium is lost. The dependence of the lifetime on the constitutive parameters is shown in Tables 1 and 2. It is seen that the sandwich is much more sensitive to variations in these parameters than is the hinge model. For materials displaying deformation Fig. 5 and Fig. 10 show that the critical state is reached after a considerably smaller deformation in the sandwich model than in the hinge. This indicates that the sandwich model gives a safer design than does the hinge model.

Acknowledgement—The author wishes to express his gratitude to Professor Jan Hult for valuable and stimulating discussion during this work.

REFERENCES

1. P. O. Boström, Creep buckling considering material damage. *Int. J. Solids Structures* **11** (1975).
2. P. O. Boström, An analysis of the effect of tension induced damage on creep buckling of columns. *Int. J. Solids Structures* **12** (1976).
3. J. Hult, Creep buckling of plane frameworks. *Proc. Durand Centennial Conference*, pp. 227–246. Standord University (1960).
4. F. R. Shanley, Inelastic column theory. *J. Aeronaut. Sci.* **14**, (1947).
5. N. J. Hoff, Buckling and stability. *J. Roy. Aer. Soc.* **58**, (1954).
6. F. K. G. Odqvist and J. Hult, *Kriechfestigkeit Metallischer Werkstoffe*. Springer, Berlin (1962).
7. H. Broberg, A new criterion for brittle creep rupture. *J. Appl. Mech.* **41**, 809 (1974).